

Systematic study of the exchange interactions in Gd-doped GaN containing N interstitials, O interstitials, or Ga vacancies

Alexander Thiess,^{1,2} Stefan Blügel,³ Peter H. Dederichs,³ Rudolf Zeller,² and Walter R. L. Lambrecht¹

¹*Department of Physics, Case Western Reserve University, Cleveland, Ohio 44106-7079, USA*

²*Institute for Advanced Simulation, Forschungszentrum Jülich and Jülich Aachen Research Alliance (JARA), D-52425 Jülich, Germany*

³*Peter-Grünberg Institut, Forschungszentrum Jülich and JARA, D-52425 Jülich, Germany*

(Received 2 June 2015; revised manuscript received 4 August 2015; published 17 September 2015)

Using large supercells models and the KKRnano multiple scattering approach, statistically meaningful information is obtained on the distribution of local densities of states, magnetic moments, and distance-dependent exchange interactions for interstitial N or O or Ga vacancies in Gd-doped GaN. The exchange interactions between N interstitials (N_i) and N_i with Gd are found to be short-ranged and mainly antiferromagnetic, while exchange interactions between Gd are negligible. For O interstitials, the ferro- and antiferromagnetic interactions between Gd and O_i are roughly canceling each other, and the O_i - O_i interactions are ferromagnetic but very short-ranged. The Fermi level dependence of these interactions is studied. The difference between N_i and O_i behavior is related to the filling of up and down spin partial densities of states, which promotes antiferromagnetic superexchange and ferromagnetic double exchange for N_i and O_i , respectively. On the other hand, Ga vacancies provide significantly stronger and more robust ferromagnetic interactions between moments localized on N near the vacancies and may reach the percolation threshold for concentrations of order 5%. The role of strain in films grown under different conditions on the vacancy concentration is discussed.

DOI: [10.1103/PhysRevB.92.104418](https://doi.org/10.1103/PhysRevB.92.104418)

PACS number(s): 75.50.Pp, 75.30.Hx, 71.70.Gm

I. INTRODUCTION

The magnetic properties of Gd-doped GaN have attracted significant attention since the claim of colossal magnetic moments and the occurrence of ferromagnetism above room temperature in extremely dilute samples at the parts per million level [1,2]. While ferromagnetism in higher concentration (of order 3%–12%) Gd-doped GaN was established earlier [3,4] and has since been further pursued and shown to arise from carrier-mediated interactions between localized Gd moments and promoted by n-type doping [5–12], the case of extremely dilute doping remains controversial.

It soon became clear that the origin of the magnetism and moments of order $4000\mu_B$, much larger than the nominal Gd^{3+} moment of $7\mu_B$, must arise from defects caused by the introduction of Gd either during growth or by implantation. In that sense, the study of magnetism in these samples is closely related to the possibility of defect or d^0 magnetism. Evidence for the role of defects came from the observation that implantation leads to even larger moments than introduction of Gd during growth and the fact that annealing decreased the moments [13,14]. Thus the more disorder, the higher the magnetic moments per Gd. Second, x-ray magnetic circular dichroism (XMCD) of the Gd edge showed that the local Gd moments behaved paramagnetically while the overall magnetization as measured by SQUID (superconducting quantum interference device) showed hysteresis [15,16].

The question then turned to which defects are responsible for the magnetism and how they are coupled to the Gd. Liu *et al.* [17] proposed that Ga vacancies provide $3\mu_B$ per vacancy in acceptor-like states above the valence band maximum (VBM), which through N- p -Gd- $3d$ coupling would explain the ferromagnetism and enhanced moments. A similar model was proposed by Dev *et al.* [18]. They found antiferromagnetic (AFM) coupling between neutral V_{Ga} but ferromagnetic (FM) coupling between V_{Ga}^{-1} or V_{Ga}^{-2} which carry respectively $2\mu_B$

or $1\mu_B$ magnetic moment. While their model did not include Gd, they proposed that these vacancies could contribute to the magnetism in this system. The vacancy model was further pursued by Gohda and Oshiyama [19]. They studied cells up to 576 sites including 71 vacancies and found the magnetic moment to linearly increase with the number of Ga vacancies. They found FM coupling between Gd and V_{Ga} but mixed FM and AFM couplings between V_{Ga} pairs, depending on the exact positioning in the lattice relative to each other.

None of these papers addressed the question of the energy of formation of Ga vacancies, which was known already to be among the higher formation energy native defects, especially in the neutral charge state which carries the highest magnetic moment [20,21]. This led Mitra and Lambrecht [22] to question the vacancy model. Besides the objection of high energy of formation, they pointed out that in typical Gd-doped samples which are semi-insulating, the Fermi level is expected to be in the middle of the gap, in which case, the Ga vacancy is in a triple negative charge state without magnetic moment. As an alternative, they proposed that N or O interstitials near the Gd could provide additional magnetic moments and found them to be coupled ferromagnetically. Interstitials were also known to occur in the implantation case through simulations of the implantation process [13,14].

None of above studies provided a systematic study of the exchange interactions as function of distance, perhaps with the exception of Gohda and Oshiyama [19]. Even in that study the exchange interactions were extracted from comparing the total energy differences of a relatively small sampling of different magnetic configurations. In that approach, one makes assumptions that the exchange interactions with farther away magnetic sites in other unit cells are negligible. This is known in several cases to overestimate the exchange interactions [23,24]. The linear response approach [25] on the other hand makes no such *a priori* assumptions. It is usually implemented in a multiple scattering approach, such

as the Korringa-Kohn-Rostoker (KKR) method and gives the exchange interaction as

$$J_{ij} = \frac{1}{4\pi} \int^{\epsilon_F} d\epsilon \text{ImTr}\{\Delta t_i(\epsilon) G_{ij}^{\uparrow}(\epsilon) \Delta t_j(\epsilon) G_{ji}^{\downarrow}(\epsilon)\}, \quad (1)$$

with $\Delta t_i = t_i^{\uparrow} - t_i^{\downarrow}$, with t_i^{σ} the on-site t matrix describing the scattering and G_{ij}^{σ} the Green's function connecting site i to j for a given spin. The trace is over angular momenta. In a periodic model, it actually provides the $J_{ij}(\mathbf{k})$ and through a Fourier transform the $J_{i,j+\mathbf{T}}$ between an atom i and an atom j in the unit cell translated by a lattice vector \mathbf{T} . Thus it allows one to determine long-range exchange interactions beyond the size of the unit cell. Furthermore, it obtains all of them from a single self-consistent calculation for a given distribution of magnetic sites in the model unit cell. The J_{ij} here are defined through the classical Heisenberg model:

$$H = - \sum_{i \neq j} J_{ij} \mathbf{e}_i \cdot \mathbf{e}_j, \quad (2)$$

with \mathbf{e}_i the unit vector along the direction of the magnetic moment \mathbf{m}_i on site i , and with the magnitude of the moments already included in the definition of J_{ij} .

In the present paper, we study the exchange interactions for interstitial as well as vacancy models in Gd-doped GaN with large unit cells using the linear response approach as implemented in the KKRnano code [26]. The large unit cells allow us to examine a realistic model with a few percent defects as well as Gd and to extract representative information on the distribution of magnetic moments and the exchange interactions.

The supercell geometries were carefully chosen to avoid extreme or rare defect configurations. Several potential supercell geometries were constructed and evaluated in terms of the defect relative distance distributions. The cells chosen for calculation were as close as possible to the theoretically calculated truly random distribution of defects. We did not consider it necessary to average over an ensemble of defect distributions because our main interest is to draw qualitative conclusions on which types of native defects could be responsible for magnetism. The chosen supercells may be considered as representative realizations of each defect type. The calculations do not include structural relaxation. The KKRnano approach is presently not suitable for relaxing the structures. The information we seek to obtain on the range of exchange interactions and distribution of magnetic moments should not be crucially affected by this idealization of the models.

We find that interstitial N has only weak and short-ranged and mostly AFM couplings. This is shown to arise mostly from the superexchange between well separated occupied majority and empty minority spin states in the defect-induced levels. Oxygen interstitials provide slightly stronger tendency toward FM interactions but still provide no viable route to explaining overall ferromagnetism in the system. It shows that a previous study [22] was too restrictive in placing interstitials only as immediate neighbors to the Gd.

Only Ga vacancies provide a route to explaining extended magnetism. A key point here is that the magnetic moments occur not on the vacancy site but on the neighboring N

atoms. Even for 4th-neighbor vacancies, the N neighbors of the vacancy are within a short enough distance of each other to allow for a significant ferromagnetic exchange interaction. This leads to a lower percolation threshold.

In a previous paper we already pursued this idea further [27]. In order to explain why vacancies can stay neutral and thus have the maximum possible magnetic moment, one of the key objections made by Mitra and Lambrecht [22], it is necessary to consider vacancy clusters large enough to pin the Fermi level locally. It was shown in Thiess *et al.* [27] that vacancy clusters can arise during growth if the optimized surface distribution of vacancies becomes frozen in. Furthermore evidence for vacancy clusters can be found in positron annihilation studies of Roever *et al.* [28].

In our previous paper [27] we furthermore showed that the magnetic properties of clustered vacancy models differ significantly from unclustered random models. In particular, they lead to a magnetization vs temperature behavior with two temperature regimes: a low-temperature regime in which the spins in different clusters stay aligned, and a high-temperature regime in which only spins within each cluster stay aligned. Therefore, we concluded that this situation corresponds to superparamagnetism rather than ferromagnetism. A qualitative agreement with this type of temperature dependence found in experiments [2,29] was pointed out.

While our previous paper [27] was focused on the clustering aspects of the vacancies, the details of our study ruling out the interstitial models were not previously published except in the present paper's first author's Ph.D. thesis [30]. The focus of the present paper is the origin and nature of magnetism and large magnetic moments in the low Gd concentration regime through interaction with defects.

II. COMPUTATIONAL METHOD

Density functional theory in the local density approximation provides the underlying framework for our computations. To deal with the strongly correlated $4f$ -electrons of Gd, the LSDA+ U approach is used [31–34]. For a half-filled f shell as occurring in Gd, they lead to a strong separation of the majority and minority spin states well below and above the Fermi level. The values of $U_f = 8.0$ eV, $J_f = 1.2$, giving an effective $U_f - J_f = 6.8$ eV, were chosen based on previous studies of GdN [35]. In addition, a $U_d = 3.4$ eV was applied as this helps to open the gap in GdN [35]. It should be mentioned that in the present KKRnano approach, these parameters may have slightly different effects than in the linearized muffin-tin orbital (LMTO) method for which they were originally obtained, as they depend on the sphere radius and the actual atomic orbitals in the spheres one projects on. They were found to place the majority (minority) spin $4f$ levels at about -5 eV (4 eV) relative to the Fermi level, with a somewhat smaller splitting than in previous work but still significantly larger than the LDA. Since these levels are far above and below the Fermi level, their precise position is of less importance. The calculations of spin-dependent states are restricted to collinear spins.

The electronic structure calculations were performed using the KKRnano approach as presented in Ref. [26]. Some important points about this method are that it is a full-potential

all-electron method. It uses the screened KKR approach, in which the structure constants are short range. The atoms are represented by Voronoi polyhedra rather than muffin-tin spheres, and no spherical approximations are made to the potential. The KKRnano approach is a Green's function method which uses special iterative techniques to solve the Dyson equation efficiently on a complex energy contour for large systems. In the present case, the energy contour used 44 energy points, 7 Matsubara frequencies, and an electronic temperature of 700 K. Furthermore it is efficiently parallelized and implemented for the architecture of a Blue Gene computer. The zinc-blende structure was chosen for the underlying GaN lattice and empty Voronoi polyhedra were placed on interstitial sites. These can then be readily replaced by interstitial atoms. Ga $4s$, $4p$, $3d$, N $2s$, $2p$, and Gd $6s$, $6p$, $5d$, and $4f$ are treated as valence states within the energy integration contour used to obtain charge densities. The angular momentum cutoff was set at $l_{\max} = 3$.

Supercells of 512 atoms or 1024 Voronoi sites were used. These are $4 \times 4 \times 4$ supercells of the conventional cubic cell of 8 atoms or 16 sites. The interstitials, Gd, and vacancies are placed randomly in these models as detailed in the results section. The coordinates of the atoms in the models used in the calculations are available in the Supplemental Material [36].

III. RESULTS

A. N interstitials

The supercell used for these calculations has composition $\text{Ga}_{248}\text{Gd}_8\text{N}_{256}(\text{N}_i)_{32}$ with the interstitials placed randomly in the two possible sites, either surrounded by other N (tetrahedral site) or by Ga (octahedral site) as nearest neighbors. These are labeled I_N and I_{Ga} respectively. The latter should not be confused with interstitial Ga, which was not studied here. The supercell studied corresponds to 3.125% of the cation sites replaced by Gd and 6.125% interstitial sites being filled with N. These are rather large percentages, not chosen to represent typical samples but rather to allow us to study the statistics of the defect characteristics meaningfully.

In Fig. 1 we show the projected densities of states (PDOS) on the interstitial N atoms in the gap region. We can see that (1) these interstitials indeed create levels in the middle of the

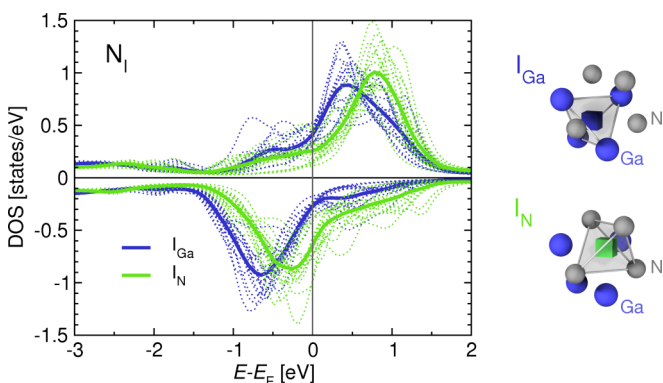


FIG. 1. (Color online) Local density of states on two types of N_i in GaN. The VBM of GaN lies at about -2 eV. The thin (dotted) lines represent individual PDOS while the thick solid line represents the average.

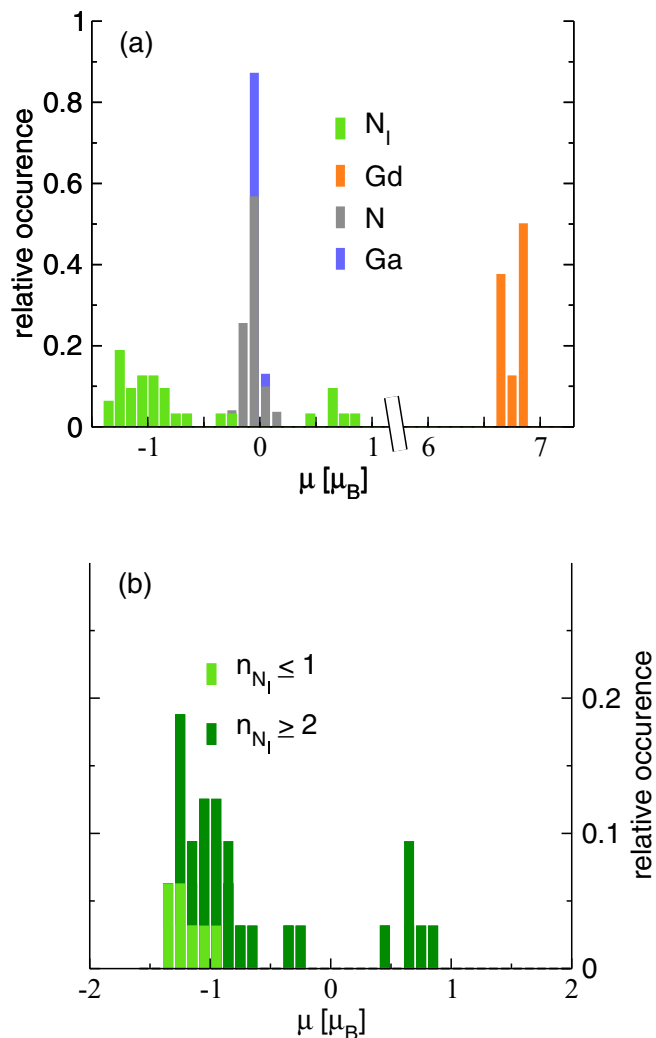


FIG. 2. (Color online) Magnetic moments in Gd-doped model with N_i : (a) relative occurrence of each magnetic moment value for Gd, N_i , lattice N, and Ga; (b) N_i separated according to how many other N_i are in the 3 neighboring shells of the N_i .

band gap, which pin the Fermi level in our overall charge neutral model, (2) there is a spread of PDOS depending on the fluctuations of the potential from site to site, (3) the averages over interstitials of each type of interstitial are distinctly shifted from each other, and (4) the up and down spin states are well separated above and below the Fermi level, respectively. The up spin here corresponds to the majority spin imposed by the Gd $4f$ states. Thus we already see that the net induced magnetic moment (area of the peak below ϵ_F) in the gap states is coupled antiferromagnetically to the Gd. In the KKR approach the total energy can be decomposed in contributions per atom. This reveals that the I_N has slightly lower energy than the I_{Ga} by 0.38 eV per site. So, interstitial N prefers the tetrahedral site.

Next, we show the magnetic moment distribution in Fig. 2. We can see that small moments (of order $<0.1\mu_B$) are induced on the lattice N and even smaller ones on Ga but the interstitial N carry a distinct moment of about $\pm 1\mu_B$. These can further be separated into two groups, the N_i which have one or less

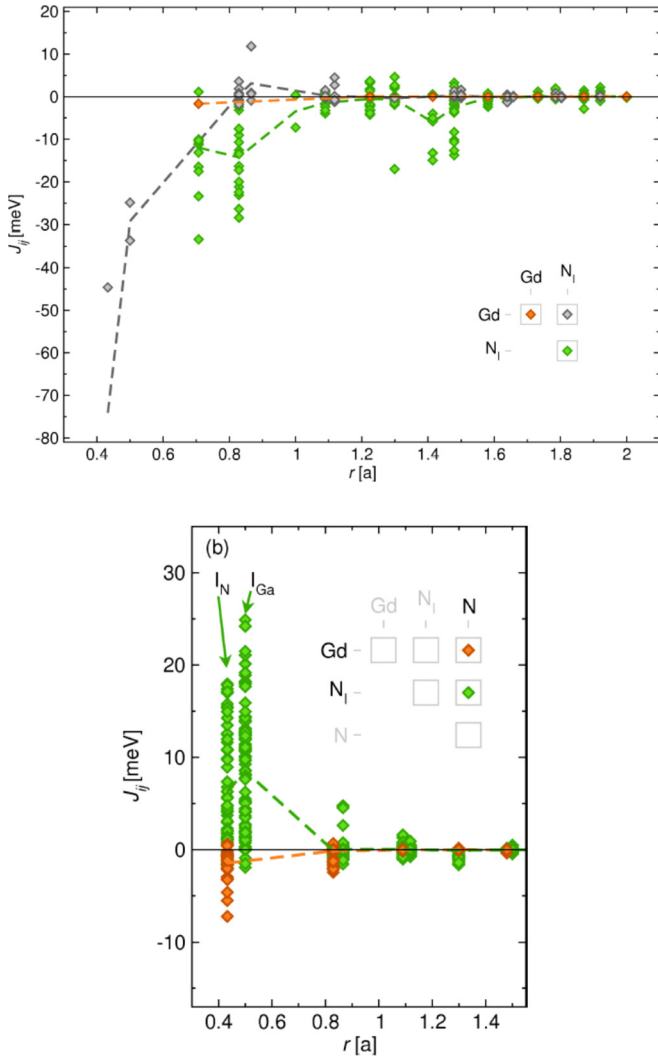


FIG. 3. (Color online) Exchange interactions for GaN:Gd with N_i . Top: Interactions between the main magnetic moment carriers. Bottom: Interactions of Gd and N_i with lattice N.

N_i in their neighborhood (defined as three shells of neighbors) and the ones that have two or more. Again, we see that the N_i moments are predominantly aligned antiparallel to the Gd moments.

The size of the magnetic moments is smaller than expected for an isolated N_i compared to Mitra and Lambrecht [22]. This is because in the KKRnano calculations, the defect levels are broadened into bands and the PDOS is smeared out due to the high-temperature broadening. This is necessary to allow for the computational speedup required in the iterative solution of the Dyson equation. However, it means that the moment is calculated as in an itinerant magnetic system by integrating the broadened PDOS up to the Fermi energy and this yields noninteger values for the moments, which are smaller than expected for isolated impurities.

The magnetic exchange interactions are shown in Fig. 3. We can see that the exchange interactions between Gd are negligible and tend to be AFM (negative). The N_i -Gd interactions are AFM at small distance and somewhat FM for larger distance but small. The N_i - N_i interactions are predominantly

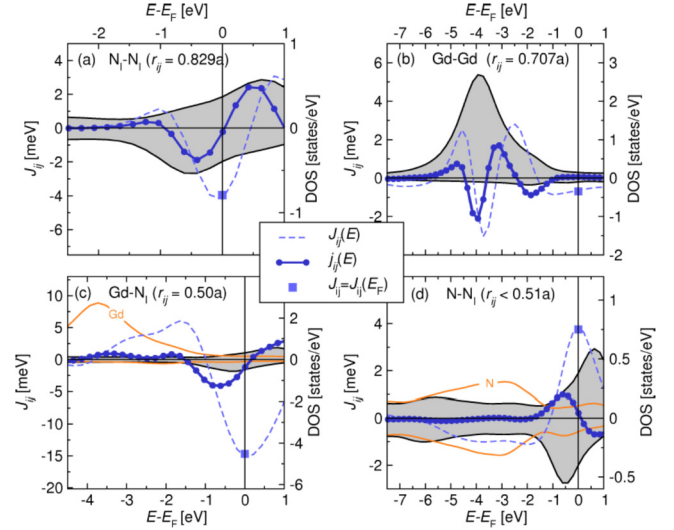


FIG. 4. (Color online) Fermi level dependence of the exchange interactions for GaN:Gd with N_i . The dashed line gives the exchange interaction, the solid line the integrand in Eq. (1), the shaded areas and orange lines represent the PDOS.

AFM. The interactions with the lattice N [shown in Fig. 3(b)] are predominantly antiferromagnetic for Gd and FM at close distance with the N_i . We may also see a large range of values for the same distance, with the mean interaction fairly small. Note again that the absolute value of the magnetic moments is already folded into the exchange interaction. The magnetic energies of interaction are obtained by multiplying these exchange interactions with unit vectors, not magnetic moments. The main conclusion is that the dominant exchange interactions between the atoms carrying the largest moments are antiferromagnetic and rather short-ranged. Thus a large buildup of a colossal magnetic moment based on interstitial N can be ruled out.

The reason for the antiferromagnetic coupling can be traced back to the electronic structure. As is well known from the Anderson-Hasegawa model [37], half-filled systems with well separated up and down spins tend to favor AFM superexchange coupling while partially filled levels for a given spin tend to favor FM coupling. For the N_i we find well separated up and down spin levels (or rather distributions of them) on both sides of the Fermi level, so the down spin states are mostly filled and the up spin states are mostly empty.

The linear response formula for exchange interactions allows us to study the dependence of the exchange interactions on the position of the Fermi level which may be controlled in principle by co-doping. Let us define $j_{ij}(\epsilon)$ as the integrand in Eq. (1). The exchange interaction is then

$$J_{ij}(\epsilon_F) = \int^{\epsilon_F} j_{ij}(\epsilon) d\epsilon. \quad (3)$$

To calculate these functions, an energy mesh just below the real axis is used with a higher electronic temperature broadening of 1600 K. The latter is required to obtain adequate convergence within the KKRnano approach. However, a large number (250) of points on the real axis are used instead of the Matsubara frequencies along the imaginary axis. In Fig. 4 we plot the

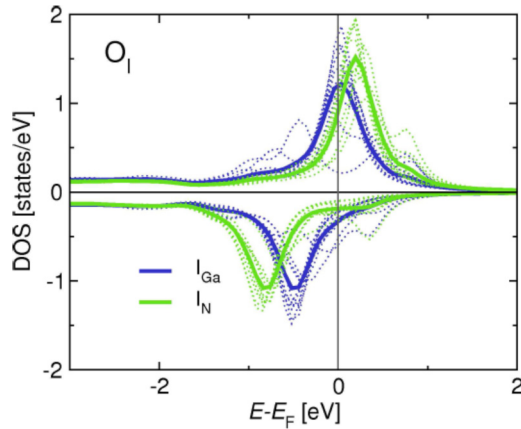


FIG. 5. (Color online) Projected density of states on interstitial O, separated according to their nearest neighbor atoms. The thin (dotted) lines represent individual PDOS while the thick solid line represents the average.

functions $j_{ij}(\epsilon)$, $J_{ij}(\epsilon)$ and the various PDOS of up and down spin (down spin is plotted as a negative PDOS as usual). In this figure we focus only on the mean short-distance exchange interactions between various types of pairs. We can see that the value of the Gd-Gd exchange is fairly robust as the $J_{ij}(\epsilon_F)$ is flat as a function of ϵ_F around its actual value. On the other hand, we can see that the N_i - N_i interaction would become less AFM for both p- or n-type doping. The same is true for the Gd- N_i interaction and the FM interaction between lattice N and N_i would also decrease under additional doping away from the system's natural Fermi level, i.e., the Fermi level corresponding to charge neutrality for the system without additional doping besides the N_i and Gd.

B. O interstitials

To model O_i interstitials, a supercell of composition $Ga_{253}Gd_3N_{256}O_{20}$ was chosen, so slightly lower Gd concentration (1.17% of cation sites) and O_i (3.9% of all interstitial sites). O_i were again randomly placed and occur in octahedral (I_{Ga}) as well as tetrahedral (I_N) sites. The PDOS on O_i in this model are shown in Fig. 5. We note, similar to N_i , the spread of PDOS depending on local potential fluctuations. Compared to N_i , the main distinction is that now the Fermi level lies close to the peak of the majority spin PDOS, in particular for the octahedral sites.

The magnetic moment histogram is shown in Fig. 6. Again, it shows small moments induced on lattice N as well as a sizable spread in O_i moments.

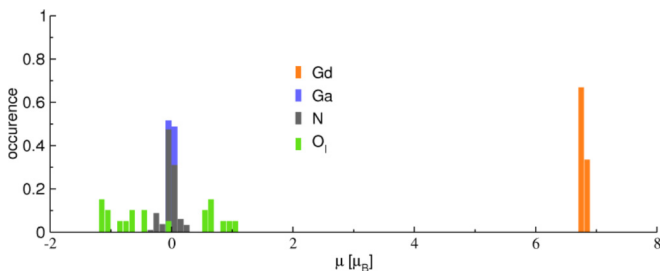


FIG. 6. (Color online) Magnetic moments in GaN:Gd with O_i .

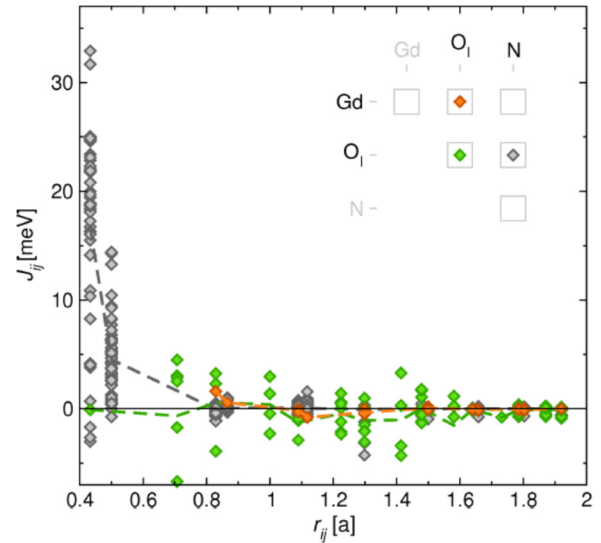


FIG. 7. (Color online) Exchange interactions for GaN:Gd with O_i .

The exchange interactions for this system are shown in Fig. 7. In contrast with the N_i , the O_i - O_i pairs have now about equal FM and AFM interactions. The interaction between Gd and O_i is also slightly more FM in character. As before the interactions of O_i with lattice N are FM at short distance. Thus, overall, one can discern a little more tendency toward ferromagnetism. However, the sizable exchange interactions are still very short-ranged. The exchange interactions become essentially negligible beyond second nearest neighbors. The reason for this trend toward FM interaction lies in the PDOS which now corresponds to partially filled spin levels.

In Fig. 8 we see that an increase in Fermi level would increase the exchange interaction while a decrease in Fermi level would decrease it because the actual Fermi level lies on an upward slope of the $J_{ij}(\epsilon_F)$ function. A comparison between N_i and O_i for the PDOS and the $j_{ij}(\epsilon)$ illustrates this further.

On the basis of the models discussed so far, we may rule out both N_i and O_i as the main sources of colossal magnetic moments or ferromagnetism in GaN:Gd. Besides, this ignores the question of why O would go in the interstitial sites instead

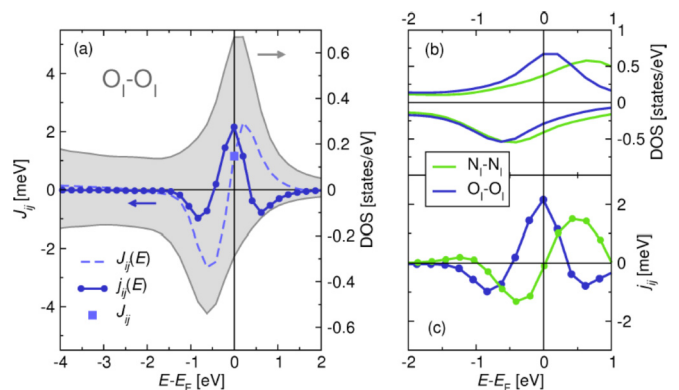


FIG. 8. (Color online) (a) Fermi level dependence of the O_i - O_i exchange interactions, (b) comparison of PDOS, and (c) $j_{ij}(\epsilon_F)$ for N_i - N_i and O_i - O_i pairs.

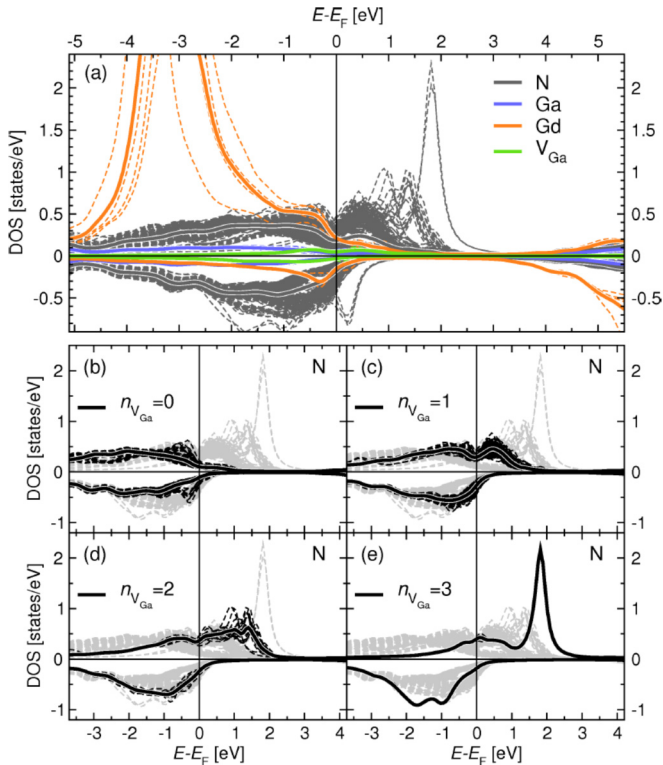


FIG. 9. (Color online) (a) Partial densities of states for GaN:Gd with V_{Ga} model. (b)–(e) show PDOS on N separated in N which are adjacent to 0–3 V_{Ga} .

of the energetically preferable substitutional site. Furthermore N_i is known to prefer a split-interstitial configuration which because of the molecular nature may be expected to have smaller magnetic moment than the unpaired N-2p orbitals in the isolated interstitials considered here. A similar O_i split-interstitial configuration was further studied by Liu *et al.* [38]. They concluded this configuration to lead to a FM situation but did not study the range of the exchange interactions and furthermore found the split interstitial to be less stable in energy than the isolated interstitials. The split interstitial was not studied here because the KKRnano approach is less suitable to deal with strongly distorted structures.

C. Ga vacancies

To study Ga vacancies, we adopt a model with composition $\text{Ga}_{220}\text{Gd}_4\text{N}_{256}$. Thus 1.56% of the cation sites were replaced by Gd and 12.5% of them were left vacant. The PDOS are shown in Fig. 9. We see states in the gap closely above the VBM. Further analysis shows that the states deeper in the gap are related to N adjacent to one or more V_{Ga} . The magnetic moment distribution (Fig. 10) shows clearly that the magnetic moment on N increases with the number of V_{Ga} it has in its nearest neighborhood. Again, these moments are smaller than expected for isolated defects because of the KKR broadening artifact mentioned earlier.

Although the vacancies were introduced randomly, we can observe a sizable magnetic domain near the region where several vacancies happened to be somewhat closer together. The magnetic moments on the N near the vacancies are shown

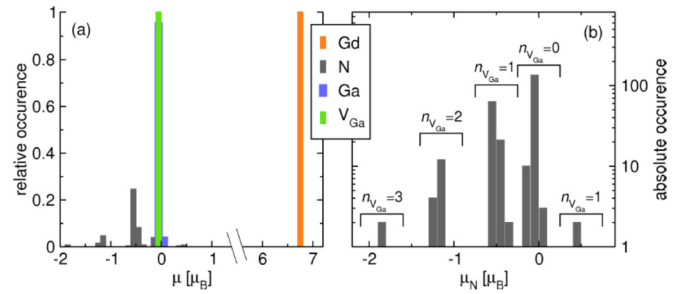


FIG. 10. (Color online) Magnetic moments for GaN:Gd with V_{Ga} .

in real space in Fig. 11. The size of the moments is here indicated by means of the size of the spheres, and the vacancies are indicated by cubes. The figure shows the absolute values rather than the direction but from Fig. 10 we see that most of the moments are in fact parallel to each other. We remind the reader that we only consider collinear spins here. Because the moments are larger on N atoms close to more than one vacancy, it is of interest to also study clustering of N vacancies. This was done in Ref. [27] where we found both evidence that vacancies may indeed prefer to cluster and second that this strongly affects the magnetic properties.

The exchange interactions are shown in Fig. 12. In this case, we see predominantly ferromagnetic interactions, although still there is a large spread around the mean interactions. Clearly, the strongest interactions are between N atoms adjacent to one or more V_{Ga} . The mean FM interaction between N adjacent to 1 V_{Ga} is about 4 meV. The higher values of the interactions are mainly from N with $n_V > 1$ which have therefore a higher moment and hence a larger J_{ij} .

The Fermi level dependence of some short-range exchange interactions in this case is shown in Fig. 13. This figure shows that the $J_{ij}(\epsilon_F)$ is at or near a peak for all of them without additional doping.

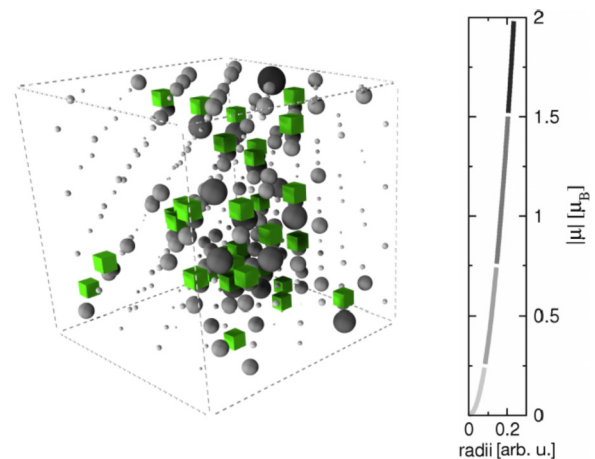


FIG. 11. (Color online) Real space distribution of magnetic moments and vacancies in the model. Vacancies are indicated by squares and magnetic moments by spheres with size according to their absolute value.

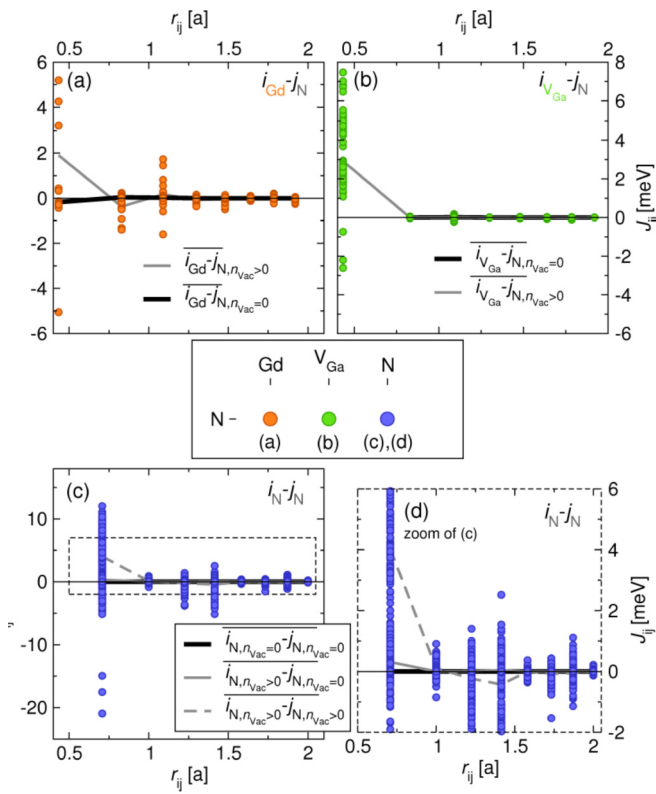


FIG. 12. (Color online) Exchange interactions for GaN:Gd with V_{Ga} . (a)–(d) show respectively interactions between Gd and N (adjacent to vacancies), V_{Ga} with N and N-N sorted according to how many V_{Ga} they are neighbor to.

IV. DISCUSSION

A. Strain aspects

Clearly, from the previous section, V_{Ga} is more promising as an explanation for defect-induced magnetism in GaN:Gd than interstitials. There remains of course the objections that

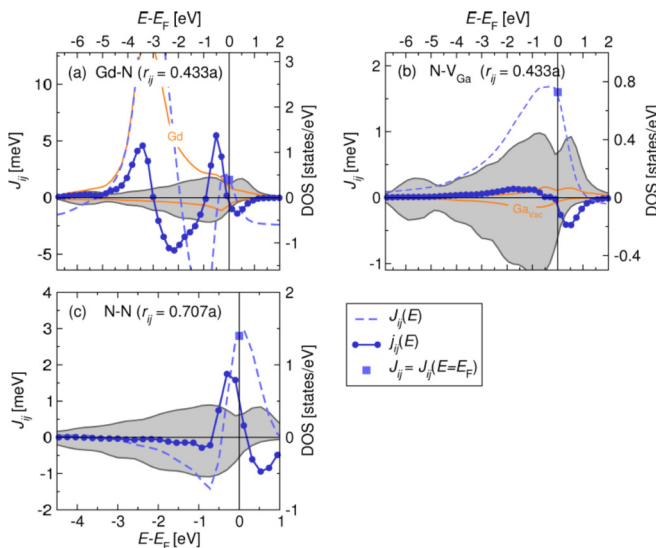


FIG. 13. (Color online) Fermi level dependence of exchange interactions in GaN:Gd with V_{Ga} .

the Ga vacancy is a high formation energy defect in its neutral charge state. We have already partially addressed this issue in a previous paper [27]. First of all, if the vacancies are clustered and form a sufficiently large local void, then they can locally pin the Fermi level and keep the defects in the neutral charge state. In contrast, isolated vacancies are more likely to be in a negative charge state with smaller or even zero magnetic moment unless the system is heavily p type so that the Fermi level stays pinned close to the VBM. Second, we showed in Ref. [27] that given a certain concentration of vacancies, they will tend to cluster in a growth simulation. There is ample experimental evidence for the presence of vacancies and in fact, clustered vacancies from positron-annihilation spectroscopy [28].

A further clue may lie in the strain of samples grown under different conditions. Mitra [39] calculated the lattice expansion due to Gd and the lattice constant shrinkage due to V_{Ga} . From this, it was found that in order to keep the lattice constant fixed, about 20 V_{Ga} are required per Gd. In this context, it is important to note that Dhar *et al.* [2] reported that the lattice constant c was decreased compared to pure GaN. This is unexpected for Gd incorporation since the Gd is a much larger atom. It may thus indeed indicate a significant incorporation of Ga vacancies, even overcompensating the expected increase in lattice constant due to Gd. In contrast, Asahi *et al.* [5] reported an increase in lattice constant up to a certain concentration of Gd. After that, the samples were found to contain GdN precipitates which would relieve the strain. In order to incorporate larger concentrations of Gd without GdN formation, the group of Asahi *et al.* [5] used lower temperature growth. In these samples reported by Asahi *et al.* [5] the magnetic moment per Gd is typically less than the nominal $7\mu_B$ per Gd^{3+} except at the highest concentrations in contrast to the group of Dhar *et al.* [2] which reports moments significantly exceeding those of Gd for small Gd concentrations. This might indicate that a major difference between samples of the Dhar vs Asahi group samples is the presence or absence of a large vacancy concentration.

This may further be related to the different substrates used by the two groups. Dhar *et al.* [1,2] used SiC substrates, in which case GaN is known to be under tensile strain, while the Asahi group used sapphire, in which case the GaN is known to be under compressive stress. This is due to the different sign of the thermal expansion coefficient mismatch relative to GaN. It seems plausible that the tensile stress in GaN on SiC facilitates the incorporation of Ga vacancies in order to counteract the additional tensile stress from incorporating Gd. Furthermore this may occur in an inhomogeneous fashion near the Gd. Under this scenario one expects indeed vacancy clusters near the Gd. In contrast, on sapphire substrates, under compressive stress, the Gd incorporation would allow the lattice constant to increase to relieve the tensile stress from sapphire and this may prevent incorporation of V_{Ga} .

B. Percolation aspects

Percolation is an important aspect of the magnetism in dilute magnetic semiconductors. As we have seen above both for interstitial N and O the exchange interactions are essentially negligible beyond second nearest neighbors. Even for Ga

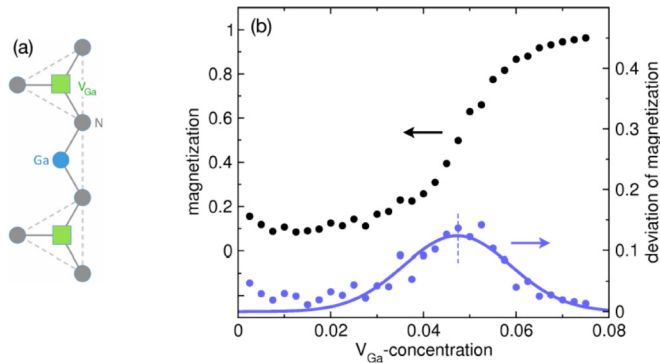


FIG. 14. (Color online) Percolation threshold for V_{Ga} in GaN. (a) illustrates that moment carrying nearest neighbor N to V_{Ga} can be nearest neighbors on the N sublattice for V_{Ga} that are 4th neighbors. (b) shows the results of a Monte Carlo model to determine the percolation threshold.

vacancies, the exchange interactions are fairly short-ranged. However, there is an important distinction. The magnetic moments with the strongest exchange interactions in this case reside on the N adjacent to the vacancy rather than on the site of the defect itself. As illustrated on the left of Fig. 14, even for V_{Ga} that are fourth neighbors to each other, their adjacent N which carry the magnetic moment are nearest neighbors on the N sublattice and within the distance for a sizable interaction. This means that the percolation threshold, the concentration for which a continuous network of interacting magnetic moments is possible throughout the sample, is set by fourth nearest neighbor distances of the vacancies. The percolation threshold on the fcc lattice [40] for fourth nearest neighbors is about 5%, while for nearest neighbors the percolation threshold on an fcc lattice is 20% [41]. The right-hand side of Fig. 14 shows our own determination of the percolation threshold for Ga vacancies. This is based on a Monte Carlo simulation of an 8000-atom cell with exclusively V_{Ga} interactions at a distance of $\sqrt{2}a$. The magnetization is shown as function of vacancy concentration. By taking the deviation of it, and fitting it to a Gaussian, one can more accurately determine the threshold concentration to occur at about 4.8%.

Keeping in mind that for the case of unchanged lattice constants, one might need 20 V_{Ga} per Gd, this threshold concentration of V_{Ga} would correspond to 0.25% Gd. It would then correspond to a magnetic moment of order $27\text{--}67\mu_B$ per

Gd. That is assuming a moment of about $1\text{--}3\mu_B$ per V_{Ga} and 7 per Gd. This is still small compared to the claimed $4000\mu_B$ per Gd but at least it provides a scenario for explaining a significant defect-induced magnetism. As was discussed in Thiess *et al.* [27] Ga vacancies tend to cluster and the magnetic properties of these clusters show that the magnetic behavior observed in such samples is more likely superparamagnetism than true ferromagnetism. The magnetic hysteresis observed to remain up to high temperatures would then be related to these clusters and may not fill the entire volume of the sample.

V. CONCLUSIONS

In this paper we studied the magnetic moment distributions and distance dependence of the exchange interactions of realistic models of Gd-doped GaN with three types of additional native defects or impurities: interstitial N, interstitial O, and Ga vacancies. The exchange interactions are found to be mostly AFM for the N_i interstitials, and mixed FM and AFM for O_i , except for very short distance interactions between O_i or N_i with lattice N. In contrast, Ga vacancies induce magnetic moments on the neighboring N, predominantly FM interactions and provide a robust path to magnetic percolated clusters because the moments in this case reside on the N neighbors of the vacancy site instead of the vacancy itself and hence allow for a lower percolation threshold. The dependence of the magnetic exchange interactions on Fermi level was studied and the nature of the exchange interactions, changing from AFM superexchange to FM double exchange, were determined. Our study was focused on the role of defect-induced magnetism in Gd-doped GaN. Besides our main results, the relation of the vacancy concentration to strain effects in Gd-doped GaN on different substrates was discussed in an attempt to explain the quite different results reported in the literature.

ACKNOWLEDGMENTS

The authors gratefully acknowledge the computing time granted by the Jülich Aachen Research Alliance, JARA-HPC Vergabegremium, and provided on the JARA-HPC Partition part of the supercomputer Blue Gene/P at Forschungszentrum Jülich. A.T.'s visit to CWRU where this work was carried out was supported by the German Academic Exchange Service (DAAD). W.L. acknowledges support from the National Science Foundation under Grant No. DMR-1104595.

-
- [1] S. Dhar, O. Brandt, M. Ramsteiner, V. F. Sapega, and K. H. Ploog, *Phys. Rev. Lett.* **94**, 037205 (2005).
 - [2] S. Dhar, L. Pérez, O. Brandt, A. Trampert, K. H. Ploog, J. Keller, and B. Beschoten, *Phys. Rev. B* **72**, 245203 (2005).
 - [3] H. Asahi, Y. K. Zhou, M. Hashimoto, M. S. Kim, X. J. Li, S. Emura, and S. Hasegawa, *J. Phys.: Condens. Matter* **16**, S5555 (2004).
 - [4] N. Teraguchi, A. Suzuki, Y. Nanishi, Y.-K. Zhou, M. Hashimoto, and H. Asahi, *Solid State Commun.* **122**, 651 (2002).
 - [5] H. Asahi, S. Hasegawa, Y. Zhou, and S. Emura, in *Magnetism and Correlated Electronic Structure of Nitrides—Rare-Earth and Transition Metals as Constituents and Dopants*, Materials Research Society Symposia Proceedings, Vol. 1290 (Materials Research Society, Warrendale, PA, 2011).
 - [6] Y. K. Zhou, S. W. Choi, S. Emura, S. Hasegawa, and H. Asahi, *Appl. Phys. Lett.* **92**, 062505 (2008).
 - [7] Y. Zhou, S. Choi, S. Kimura, S. Emura, S. Hasegawa, and H. Asahi, *Thin Solid Films* **518**, 5659 (2010).

- [8] S. N. M. Tawil, R. Kakimi, D. Krishnamurthy, S. Emura, H. Tambo, S. Hasegawa, and H. Asahi, *Phys. Status Solidi RRL* **4**, 308 (2010).
- [9] K. Higashi, S. Hasegawa, D. Abe, Y. Mitsuno, S. Komori, F. Ishikawa, M. Ishimaru, and H. Asahi, *Appl. Phys. Lett.* **101**, 221902 (2012).
- [10] M. Ishimaru, K. Higashi, S. Hasegawa, H. Asahi, K. Sato, and T. J. Konno, *Appl. Phys. Lett.* **101**, 101912 (2012).
- [11] M. Takahashi, Y. Hiromura, S. Emura, T. Nakamura, Y. K. Zhou, S. Hasegawa, and H. Asahi, *AIP Conf. Proc.* **1199**, 411 (2010).
- [12] J. Hite, R. Frazier, R. Davies, G. Thaler, C. Abernathy, S. Pearton, J. Zavada, E. Brown, and U. Himmerich, *J. Electron. Mater.* **36**, 391 (2007).
- [13] S. Dhar, T. Kammermeier, A. Ney, L. Pérez, K. H. Ploog, A. Melnikov, and A. D. Wieck, *Appl. Phys. Lett.* **89**, 062503 (2006).
- [14] M. A. Khaderbad, S. Dhar, L. Pérez, K. H. Ploog, A. Melnikov, and A. D. Wieck, *Appl. Phys. Lett.* **91**, 072514 (2007).
- [15] A. Ney, T. Kammermeier, E. Manuel, V. Ney, S. Dhar, K. H. Ploog, F. Wilhelm, and A. Rogalev, *Appl. Phys. Lett.* **90**, 252515 (2007).
- [16] A. Ney, T. Kammermeier, V. Ney, S. Ye, K. Ollefs, E. Manuel, S. Dhar, K. H. Ploog, E. Arenholz, F. Wilhelm *et al.*, *Phys. Rev. B* **77**, 233308 (2008).
- [17] L. Liu, P. Y. Yu, Z. Ma, and S. S. Mao, *Phys. Rev. Lett.* **100**, 127203 (2008).
- [18] P. Dev, Y. Xue, and P. Zhang, *Phys. Rev. Lett.* **100**, 117204 (2008).
- [19] Y. Gohda and A. Oshiyama, *Phys. Rev. B* **78**, 161201 (2008).
- [20] J. Neugebauer and C. G. Van de Walle, *Phys. Rev. B* **50**, 8067 (1994).
- [21] S. Limpijumnong and C. G. Van de Walle, *Phys. Rev. B* **69**, 035207 (2004).
- [22] C. Mitra and W. R. L. Lambrecht, *Phys. Rev. B* **80**, 081202 (2009).
- [23] M. van Schilfhaarde and O. N. Mryasov, *Phys. Rev. B* **63**, 233205 (2001).
- [24] A. Herwadkar, W. R. L. Lambrecht, and M. van Schilfhaarde, *Phys. Rev. B* **77**, 134433 (2008).
- [25] A. Liechtenstein, M. Katsnelson, V. Antropov, and V. Gubanov, *J. Magn. Magn. Mater.* **67**, 65 (1987).
- [26] A. Thiess, R. Zeller, M. Bolten, P. H. Dederichs, and S. Blügel, *Phys. Rev. B* **85**, 235103 (2012).
- [27] A. Thiess, P. H. Dederichs, R. Zeller, S. Blügel, and W. R. L. Lambrecht, *Phys. Rev. B* **86**, 180401 (2012).
- [28] M. Roever, J. Malindretos, A. Bedoya-Pinto, A. Rizzi, C. Rauch, and F. Tuomisto, *Phys. Rev. B* **84**, 081201 (2011).
- [29] L. Pérez, G. S. Lau, S. Dhar, O. Brandt, and K. H. Ploog, *Phys. Rev. B* **74**, 195207 (2006).
- [30] A. Thiess, Ph.D. thesis, RWTH Aachen, 2011.
- [31] V. I. Anisimov, J. Zaanen, and O. K. Andersen, *Phys. Rev. B* **44**, 943 (1991).
- [32] V. I. Anisimov, I. V. Solovyev, M. A. Korotin, M. T. Czyzyk, and G. A. Sawatzky, *Phys. Rev. B* **48**, 16929 (1993).
- [33] A. I. Liechtenstein, V. I. Anisimov, and J. Zaanen, *Phys. Rev. B* **52**, R5467 (1995).
- [34] V. I. Anisimov, F. Aryasetiawan, and A. I. Liechtenstein, *J. Phys.: Condens. Matter* **9**, 767 (1997).
- [35] W. R. L. Lambrecht and P. Larson, in *Advances in III-V Nitride Semiconductor Materials and Devices*, Materials Research Society Symposia Proceedings, Vol. 955 (Materials Research Society, Warrendale, PA, 2006).
- [36] See Supplemental Material at <http://link.aps.org/supplemental/10.1103/PhysRevB.92.104418> for the coordinates of the atoms in the models used in the calculations.
- [37] P. W. Anderson and H. Hasegawa, *Phys. Rev.* **100**, 675 (1955).
- [38] Z. Liu, X. Yi, J. Wang, J. Kang, A. G. Melton, Y. Shi, N. Lu, J. Wang, J. Li, and I. Ferguson, *Appl. Phys. Lett.* **100**, 232408 (2012).
- [39] C. Mitra, Ph.D. thesis, Case Western Reserve University, 2009.
- [40] K. Sato, L. Bergqvist, J. Kudrnovský, P. H. Dederichs, O. Eriksson, I. Turek, B. Sanyal, G. Bouzerar, H. Katayama-Yoshida, V. A. Dinh *et al.*, *Rev. Mod. Phys.* **82**, 1633 (2010).
- [41] S. Kirkpatrick, *Rev. Mod. Phys.* **45**, 574 (1973).